Use of antiscalant polymers in industrial cooling circuits: laboratory local inhibition law applied to the modeling of a pilot plant performance

Norinda Chhim, Thibaut Neveux, Céline Bouteleux, Sébastien Teychené, Béatrice Biscans

Use of antiscalant polymers in industrial cooling circuits: laboratory local inhibition law applied to the modelling of a pilot plant performance

Norinda Chhim[a,b], Thibaut Neveux[a], Céline Bouteleux[a], Sébastien Teychené[b], Béatrice Biscans[b*]

[a] EDF Lab Chatou, 6 Quai Watier, 78401 Chatou Cedex, France

[b] Laboratoire de Génie Chimique, Université de Toulouse, CNRS, INPT, UPS,

4 Allée Emile Monso CS84234, 31432 Toulouse, France

Corresponding author: beatrice.biscans@toulouse-inp.fr

Abstract

Calcium carbonate scaling in industrial cooling circuits is a serious problem limiting the efficiency of heat exchanges. One preventive treatment consists in injecting an inhibitor polymeric additive in the circulating water. This work focuses on scaling experiments carried out in pilot plants, with and without additive, and simulated by using the CooliSS software (Cooling circuit Simulation Software) developed by EDF company. A local inhibition law of $CaCO_3$ crystal growth describing the adsorption of additive was found and implemented to calculate the global variation of calcium in the pilot plant. A small quantity of additive rapidly results in a decrease of the calcium deposit. The presence of suspended solids in water decreases the global inhibition by adsorption on other solids than calcite (illite, SiO2). It was shown that the efficiency factors (inhibition ratios) depend on the nature of the surface (material) and on the presence of suspended particles in the cooling water.

Keywords:

Precipitation, Pilot plant, scale inhibition, cooling circuit, calcium carbonate

1. INTRODUCTION

Fouling is a complex and unwanted process where material from the environment, such as suspended particles or precipitated species adhere to a surface. This process causes problems in medical, marine, oil and gas industry and scale inhibitors are often used to mitigate this unwanted phenomenon (addition of antiscalant delays the scaling). Calcium and magnesium ions are the major components of scaling in different water sources. Several previous studies were focused on new experimental or modelling methodologies to rapidly evaluate the antiscaling potential of new additives under different application conditions, in order to provide more efficient technologies for scale control [1,2]. Among the many research group working on the development of various antiscalant and their efficiencies for scale inhibition, some considered high concentration of feed water and high temperature on the inhibition mechanism and showed that a higher dose of antiscalant was required to inhibit the scale formation for the relatively higher concentration of seawater and at a higher temperature [3]. Recently, green

additives such as Bistorta Officinalis extract were also tested as inhibitors for prevention of corrosion and scale formation problems in cooling water system [4]. The inhibition action of this extract is due to adsorption of insoluble Fe^{2+} complexes over the steel surface and behaves as a mixed-type film forming corrosion inhibitor and prevent scale formation.

The modeling of scale inhibition can be done using experiential data based on the RSM (Response Surface Methodology) and analysis of variance (ANOVA) such as in oil field treatment [5] or it can be based on mechanistical approaches [6].

Industrial cooling circuits are subject to fouling and deposit of mineral particles such as calcium carbonate ($CaCO_3$) associated to the suspended matter naturally present in cooling waters. This phenomenon can lead to layers of hard scale, increasing heat transfer resistance and thus impairing heat exchange. This is a serious problem in industry, especially in high energy consumption equipment such as industrial cooling systems [6,7].

In such cooling circuit, water is usually taken directly from the natural environment (river) and due to the presence of various chemical elements (ions, mineral salts and dissolved or suspended substances such as colloids, clays) chemical fouling (scale deposit) and physical fouling (scale deposit associated with suspended matter) occur on the surface of the heat exchange bodies. This is due to the evaporation of water in the atmospheric refrigerants resulting from the operating conditions of the cooling circuits. This evaporation leads to a concentration increase of certain dissolved salts, in particular calcium and bicarbonate, but also of other materials naturally present in river water such as suspended solids (SS) and organic matter. The increase of the concentration of these main elements results in the modification of chemical equilibria leading to the crystallization of dissolved salts and the deposits of SS on the surfaces of the exchange body (metal tubes of the condenser, PVC cooling tower packings). In addition, the rise of water temperature at the outlet of the condenser, kinetically (by increasing the reaction kinetics) and thermodynamically (by reducing the solubility) promotes the precipitation of calcium carbonate.

The mechanisms of scale deposits in a semi-closed industrial cooling circuit are complex because they result from the coupling of many physicochemical and operating parameters:

- water quality (supersaturation, SS, organic matter, pH)
- circuit operating conditions (temperatures, volume concentration factor (F_{VC}), hydrodynamics of the flow, residence time)
- type of exchanger materials (nature, surface topology).

Hence, there is a strong need to find ways to minimize fouling. One way is to incorporate antifouling polymers in the circulating water. Indeed, a polymeric antiscalant can suppress scale formation with very low dosage and hence, at an affordable cost. The scale inhibition mechanism involves complex phenomena related to transport of the inhibiting molecules from the solution bulk to the scaling surface or to the suspended existing particles. This is followed by adsorption/reaction of the molecules with active growth sites of the scale matrix thus interfering with nucleation and crystal formation processes [8,9,10]. However, the scale deposit inhibition efficiency generated by the presence of polymeric additive such as homopolymer of acrylic acid (HA), polyepoxysuccinic acid (PESA) or polyaspartic acid (PASP) is influenced by [11]:

- the additive concentration,

• the temperature of the circulating water in the cooling system which has an impact on the growth inhibition kinetics,
• the presence of SS in the system and the heat exchange body materials impacting the amount of polymeric additive.

The studies proposed in the literature mainly focus on comparing the efficiency of polymers with each other, at the laboratory scale, such as in the work of D. Liu [12]. Sometimes the identification (without quantification) of inhibition mechanisms are discussed [13], but relatively little is found on modeling the efficiency, operating with natural river water and at the industrial scale. Neveux et al. [6] have conducted experiments in a pilot plant using raw river water and provide a comprehensive knowledge on the antiscalant efficiency of polymers, showing that crystal-growth inhibition of calcite occurs rather than nucleation inhibition. This was attributed to the high supersaturation level and long residence times in the system. Some other studies are related to modeling of polymer efficiency (or the calculation of the minimum dose) for inhibiting scaling and a non-exhaustive list is given in table 1.

Authors	**Used for**	**Expected effect: Nucleation Inhibition**	**Expected effect: Growth inhibition**	**conditions**
Puckorius, cited par R.R. Cavano [14]	Prevention	Yes: Minimum dosage depends on the water hardness	yes	Industrial experience feedback
S. He *et al.* [15,16]	Prevention	Yes: calculation of a minimum dosage	yes	Laboratory study Synthetic water
R. J. Fergusson *et al.* [17]	Prevention	Yes: increase of induction time	No	Laboratory study + industrial tests Synthetic water + process
D. Vanderpool [18]	Prevention	Yes: calculation of a minimum dosage	yes	unspecified
D. Lisitsin *et al.* [10]	Slow down	No effect	Yes (adsorption)	Laboratory study Synthetic water
T.Neveux et al. [6]	Slow down	No	Yes	Industrial Pilot plant
Chhim et al. [7]	prevention	Yes : increase the induction time	Yes	Laboratory constant composition method

Table 1: Some previous works focused on polymers efficiency modeling, at the laboratory scale or at the industrial scale

The results of Puckorius reported by Cavano [14] indicate orders of magnitude of inhibitor dosage to be injected as a function of classical saturation indexes (Langelier, Ryznar, Puckorius) for three inhibitors: 1-hydroxyethane1,1-diphosphonic acid, phosphonobutane-tricarboxylic acid and polyacrylic acid. No theoretical consideration was used and these orders of magnitude were only based on experience feedback and do not consider operating conditions such as the actual circuit level of temperature or circuit volume concentration factor F_{VC}. They were therefore not easily transposable from an industrial system to another.

The work of S. He et al. [15, 16] proposed a nucleation inhibition model by measuring the differences in induction time obtained with and without scale inhibitor, using the classical kinetic law of nucleation. In the case of scale control, the objective is to extend the induction time until a water has safely passed through the cooling system. The authors thus observed experimentally that the calculated interfacial energy was proportional to the amount of inhibitor injected. They deduced the dose of inhibitor to be injected as a function of the water supersaturation index, temperature and induction time desired to protect the system during the residence time of the water in the circuit.

Similarly, Fergusson et al. [17] proposed a model to calculate an induction time. They observed that this time varies with the inhibitor concentration (commercial phosphonate) for different precipitates (calcite, gypsum, barite, celestite, silica, calcium phosphates). This model was implemented in the "Water Cycle" software which calculates a minimum dose of inhibitor.

D. Vanderpool [18] also proposes a minimum dose calculation based on 3 terms: a homogeneous nucleation term (similar to the previous authors), a term corresponding to the quantity of inhibitor adsorbed on surfaces, and a term representing the amount of inhibitor necessary to maintain the adsorption equilibrium (prevent desorption of the polymer). Thus, the effect of suspended solids (SS) and circuit materials were taken into account via adsorption coefficients and specific surface areas. Values are given for several inhibitors (1-Hydroxyethylidene-1,1-diphosphonic Acid (HEDP), 2-Phosphonobutane-1,2,4, -tricarboxylic Acid (PBTC), Polyamino Polyether Methylene Phosphonic Acid (PAPEMP)).

By neglecting the phenomenon of homogeneous nucleation, Lisitsin et al. [10] focused their work on surface reaction leading to crystal growth and proposed a model of adsorption of polymeric inhibitor molecules, occupying active growth sites. Their approach was developed for commercial phosphonate-based inhibitors (Permatreat PC 191, Calgon SHMP, Coatex E 201, Genesys LS). The effect of temperature was not investigated while the adsorption mechanism is strongly favored at lower temperature.

Finally, studies focus mainly on nucleation and little on growth and they are often carried out at the laboratory scale with synthetic waters. This is probably linked to the fact that the concerned industries use open systems for which the extension of the induction time to a value greater than the time the water passes through the industrial circuit, is sufficient.

Recent studies proposed green polymer inhibitors against $CaCO_3$ scaling [7,19]. Among the possible green anti-scalants, polyepoxysuccinic acid (PESA) and polyaspartic acid (PASP) have proven to be green corrosion scale inhibitors given their non-nitrogenous, non-phosphorus, and biodegradable features [20].

In previous studies Chhim et al., [7], adapted the constant composition method at the laboratory scale, for calcium carbonate precipitation, in order to replicate experimentally the operating conditions of industrial recirculating cooling water systems, especially with respect to the supersaturation range, presence of suspended matter (such as illite, silica, calcite) and the temperature range encountered. In their study, this constant composition method precipitation (constant supersaturation, pH and ionic force) was applied to investigate the influence of polyepoxysuccinic acid (PESA), polyaspartic acid (PASP) and their mixture and to compare the inhibition results to homopolymer of acrylic acid (HA), a classical polymeric additive. So, scaling inhibition performance was investigated through dynamic constant composition

precipitation experiments to obtain $CaCO_3$ growth kinetics in conditions representative of an industrial circuit.

Their results showed that when HA was added to the growing medium, no crystallization delay was observed, but crystal growth was strongly slowed down. With the addition of PASP, a slight increase of delay time was observed and crystal growth on calcite seeds was also strongly slowed down. Unlike to the other two polymers, PESA acts differently: no inhibition of crystal growth but strong inhibition of nucleation. The three additives tested in this previous study (HA, PASP and PESA) show three different action ways, that explain the synergetic effects found when two additives were mixed. A mixture of PESA and PASP provided a promising approach for scale inhibition. Under the experimental conditions applied in this study [7], maximum apparent delay time was nearly 19 hours, with inhibition rate close to 89% for a mixture of PESA at 1.5 mg $\cdot L^{-1}$ and PASP at 0.5 mg $\cdot L^{-1}$. In comparison, mean residence time in industrial cooling circuits is around 24 hours; thus, a PESA-PASP mixture (both green additives) should significantly reduce scaling by acting on nucleation and crystal growth. In addition, the formation of aggregated vaterite particles with pumpkins shape make the deposit more porous and thus less adherent to the surface.

This paper intends to bridge the gap between the inhibition efficiency obtained through laboratory measurements in controlled conditions and through process scale measurements (pilot-plant or industrial systems) for the same conditions of supersaturation, nature and quantity of suspended particles.

To do so, the local growth kinetics laws and inhibition obtained at the laboratory scale in the constant composition experiment [7] are validated by local measurements performed in an industrial pilot plant. An adsorption-based model was then proposed to quantify the inhibition of precipitation kinetics with respect to the process operating conditions and water qualities. This law was then implemented in the CooliSS software (Cooling circuit Simulation Software) in order to simulate the efficiency of a polymeric additive (homopolymer of acrylic acid (HA)), at the scale of the industrial cooling circuit system. The results of the simulation by CooliSS were compared to experimental measurements performed in an industrial pilot plant. Indeed, this comparison makes it possible, to validate the efficiency of a polymeric additive at the scale of the pilot plants obtained by the calcium inlet / outlet balance. This paper also provides new experimental data on the influence of suspended matter, additive concentration and temperature; both at local scale (kinetic) and global scale (inlet / outlet mass balance) of the industrial pilot plant.

2. MATERIAL AND METHODS

2.1. Pilot plant description

In this work two pilot plants located in the EDF Lab Chatou research facility on the Seine river (in France) were used (Figure 1). Each pilot plant is mainly composed of a low-pressure steam condenser (with a heat load up to 24 kW_{th}), a counter-current cooling tower, an ambient air fan equipped with humidity and temperature control, a washing tower, hot and cold tanks, a

recirculation pump, and injections pumps for various additives (e.g., acids, polymers, and biocides). The pilot plant (at 1/140000 scale of the industrial power plant, i.e. constructed from one condenser tube) is designed to be representative of hydrodynamics and water chemistry of the cooling circuit of the power plant. The set-up is also representative of materials used in the main active components as the same metals are used in the condenser tube (e.g., stainless steel) and for the cooling tower packing (e.g., structured PVC); ducts, and tanks are nonetheless made of plastic instead of concrete.

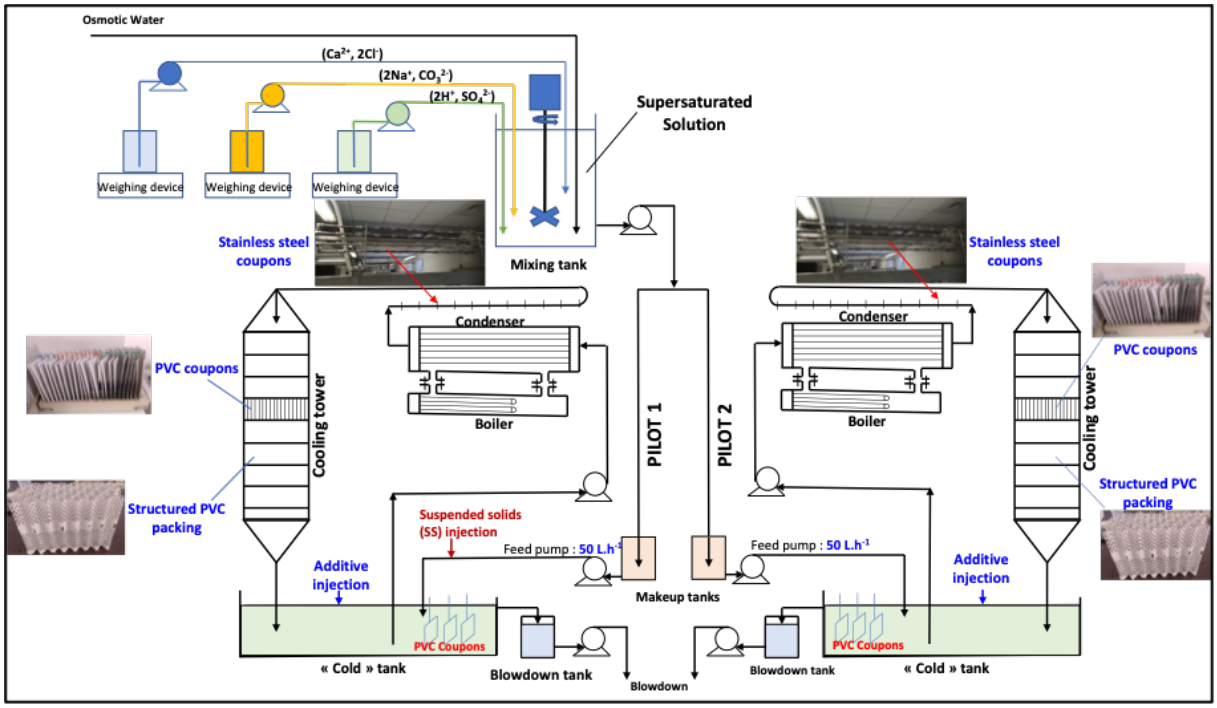

***Figure 1**: Pilot plant set-up in EDF company, used in this work and location of the coupons (local scaling on samples of materials) in the twin pilot plants*

Three main dependent elements of the pilot plant will be followed during the experiments (Figure1):

• the condenser made up of metal tubes is supplied with water partly coming from the "cold" tank and another part from "fresh" extra water drawn from the river. This extra water makes it possible both to compensate the evaporation in the atmospheric refrigerant and to ensure an acceptable chemical composition of the water in the industrial cooling system. After passing through the condenser, the water leaving at a temperature of 35 to 45°C is returned to the atmospheric refrigerant to be cooled. The cooling cycle is repeated.

• the atmospheric refrigerant in which PVC packings are generally used in order to increase the countercurrent exchange surface between the water to be cooled and the rising air. During this cooling operation, part of the water is evaporated leading to an increase in the concentrations of chemical species and also suspended solids (SS), in particular the precursor salts for the formation of the $CaCO_3$ deposit.

• the "cold" tank in which the cooled water is collected. In order to control the concentration of the chemical species accumulated in the cooling circuit, part of the water from the “cold” tank is purged into the river.

To characterize the overconcentration of chemical species entering the cooling system, it is usual to consider the ratio of the makeup water flow rate to the blowdown flow rate, called volume concentration factor (F_{VC}).

2.2.Operating conditions

The two identical pilot plants were used in parallel. They are preliminary pre-scaled with a supersaturated solution without any suspended solids (SS). Then, one pilot plant is used with water initially free of suspended particles (PILOT1) and the other (PILOT2) containing suspended solid particles (SS).

The two pilot plants were assigned to all the assays with an overall duration of 12 weeks. This duration was relatively short compared to the number of factors of interest to be studied and in particular compared to the time needed to observed the first layer of calcium carbonate crystals on the surfaces (9 days). So, it was decided to carry out the tests with two main parameters of interest (effects of the concentration of one single polymeric additive and of the suspended solids concentration) starting from the pilot surfaces pre-scaled exactly in the same way for the two pilot plants.

For this experimental program, the use of river water exposes its physicochemical quality to fluctuation. To avoid any fluctuation of the water quality, making it difficult to compare the results (between laboratory device with constant composition method and pilot plants), synthetic water was used with a controlled supersaturation ratio. The two pilot plants are then supplied with the same supersaturated solution, prepared from three reagents (osmotic water+ $CaCl_2$ + Na_2CO_3 + H_2SO_4) whose concentrations and injection rates in the container containing this mixture are calculated using PHREEQC software, in order to obtain a supersaturation ratio Ω of 7.6, representative of the industrial cooling circuit. The supersaturation ratio was obtained by the following equation (1):

$$\Omega = \left(\frac{a(\mathrm{Ca^{2+}})a(\mathrm{CO_3^{2-}})}{\mathrm{K_s}}\right) \qquad (1)$$

$a(\mathrm{Ca^{2+}})$ and $a(\mathrm{CO_3^{2-}})$ are the activities of the species.

All the experiments in the two pilot plants were carried out by setting a volume concentration factor (Fvc) of the installation at around 1.6. For a feed solution prepared at a supersaturation rate of $\Omega_{\text{input solution}}$ = 7.6, the supersaturation rate in the pilot plants is estimated to be about 19.5, for a circulating volume of 270 liters, by equation (2).

$$\Omega_{set-up} = F_{VC}^2\, \Omega_{input\ solution} \qquad (2)$$

To be representative of the natural water, the experiments carried out consist in adding in one of the pilot plants suspended solids at different concentrations from a "stock" solution of suspended solids typically found in rivers: calcite, silica and illite particles.

During the course of all the experimental periods in the pilot plants, some physicochemical parameters are monitored daily in each pilot plant to control the volume concentration factors and to ensure the proper functioning of the pilots. Table 2 gives the operating conditions of the experiments in these two pilot plants.

	PILOT 1	PILOT2
Water quality	$[Ca^{2+}]$ =22 10^{-4} mol.L^{-1} Ω_{makeup} = 7.6 $\Omega_{set\text{-}up} = F_{VC}^2\ \Omega_{makeup} \approx$ 19.5 pH=8.1	$[Ca^{2+}]$=22 10^{-4} mol.L^{-1} Ω_{makeup} = 7.6 $\Omega_{set\text{-}up} = F_{VC}^2\ \Omega_{makeup} \approx$ 19.5 pH=8.1
Type of Initial Suspended particles	0	Calcite 100%
		Calcite 90.3 % + silica 6.7 % + illite 3 %
Concentration of total added suspended particles	0	20 to 300 mg.L^{-1} (median diameter =30μm)
Volumetric concentration factor F_{VC}	1.6	1.6
Temperature at the outlet of the condenser	40°C	40°C
Temperature in the cold tank	30°C	30°C
Additive concentration HA (homopolymer of acrylic acid)	0 to 8 mg.L^{-1} = 0 to 4 10^{-6} mol.L^{-1}	0 to 8 mg.L^{-1} = 0 to 4 10^{-6} mol.L^{-1}

Table 2: Experimental conditions of the trials performed in pilot plant 1 and 2

2.3. Experimental methodology

Based on the knowledge acquired previously at the laboratory scale in the constant composition device, and the adsorption device [7,11], this work gives additional data acquired locally at different points in the pilot set-up, as well as the global calcium input/output level.

The overall methodology is illustrated in Figure 2. It involves both experimental and modeling activities, also both at local scale (kinetic phenomena) and global scale (process system). It is detailed in the following sections.

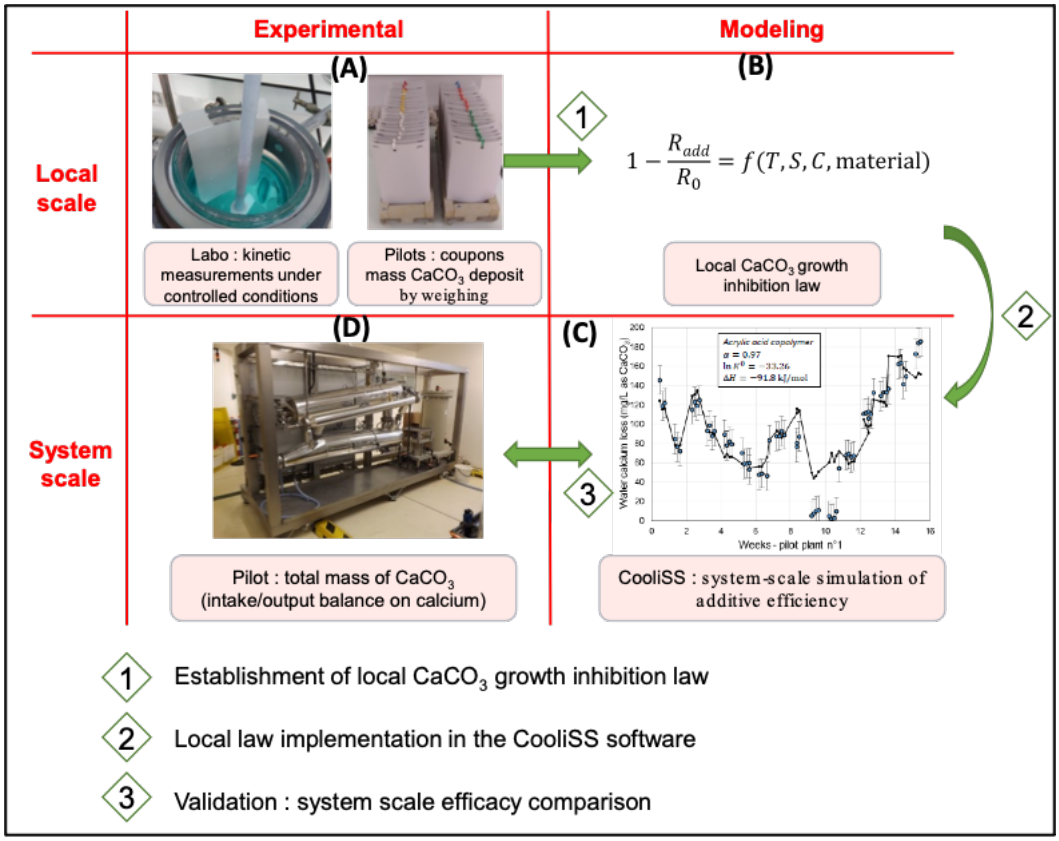

***Figure 2**: Methodology of validation and implementation of the local $CaCO_3$ growth kinetics in the global modeling of the cooling circuit.*

2.3.1. Local (phenomenological scale) inhibition efficiency

The principle consists in monitoring the evolution of the deposit mass on small rectangular surfaces introduced as samples in the pilot circuit and withdrawn during the operation, called "coupons" (figure 2(A)). So, when a polymeric additive is added in the water the local growth kinetics and inhibition growth of calcium carbonate crystals are established as a function of different factors of interest such as temperature, supersaturation, polymer concentration, type of surfaces. The average local rate R of formation of the $CaCO_3$ deposit is evaluated from the following equation:

$$R(mol.m^{-2}.min^{-1}) = \frac{m_{CaCO_3}(g)}{M_{CaCO_3}\,(g.mol^{-1})\;S\,(m^2)\;t_{exposure}\,(min)} \qquad (3)$$

m_{CaCO3} is the mass of deposit, M_{CaCO3} is the molar mass of $CaCO_3$ equal to 100.091 $g.mol^{-1}$, S represents the surface area of the material in contact with the supersaturated solution expressed in m^2 and t is the exposure time of the coupons taken in minutes.

The nature of the coupon material was representative of the type of material found in the three main parts of the pilot plant: stainless steel for the condenser, PVC in the cold tank and commercial packing (CP) in the air-cooling tower. Figure 1 shows the locations of the different types of coupons during the experimental campaigns.

The efficiency of the polymeric additive can be calculated by introducing an inhibition ratio η_{local}:

$$\eta_{local}\,(\%) = \frac{R_0 - R_{add}}{R_0} \times 100 \qquad (4)$$

R_0 (calculated from equation (3)) and R_{add} are respectively calcium carbonate growth rate obtained without and with additive.

The measured variables used to obtain the rate of formation of the $CaCO_3$ deposit, are the mass of the deposit (m_{CaCO3}) and the exposure time ($t_{exposure}$). Therefore, the local rates of formation of the $CaCO_3$ deposit on the surfaces of different coupons exposed in different locations of the pilot plant, can be determined by monitoring the weight change of each coupon as a function of their residence time. The coupons are taken out at given times and dried in an oven for 1 hour at 60 ° C, then cooled before being weighted. Then, the coupons are put back in their place after the weighing operation. In order to limit the output time of the coupons as much as possible, the drying time is limited to 1 hour.

2.3.2. Global (process system scale) inhibition efficiency

Local inhibition efficiencies expressed in equation (4) measure the effect of additive on the growth kinetic of calcium carbonate, which is a crucial phenomenological information. At global scale (process system), the relevant information is rather: how much calcium carbonate deposit is avoided thanks to the additive?

An integral indicator measuring the calcium carbonate deposit in the entirety of the process is the "calcium loss", a simple calcium balance between water input and output of the process:

$$\Delta Ca\ (°f) = (F_{VC} * THCa_{makeup}) - THCa_{blowdown} \qquad (5)$$

The water calcium hardness is measured by THCa (hydrotimetric calcium titer) and expressed in French degrees (° f) with an equivalence of 1 °f THCa equal to 10^{-4} mol. L^{-1} of Ca^{2+}; alternatively, THCa and ΔCa can be expressed in mg_{CaCO3}/L. $THCa_{makeup}$ is the concentration of Ca^{2+} in the additional container (see figure 1) and $THCa_{blowdown}$ in the blowdown and F_{VC} is the volume concentration factor (ratio of the makeup water flow rate to the blowdown flow rate).

A global inhibition ratio (η_{global}) can be calculated by the calcium input/output balance obtained in experiments without (ΔCa_0) and with additive (ΔCa_{add}):

$$\eta_{global}\,(\%) = \frac{\Delta Ca_0 - \Delta Ca_{add}}{\Delta Ca_0} \times 100 \qquad (6)$$

These expressions of water calcium loss and overall inhibition ratio are generic to any process with calcium carbonate deposition, and are obtained directly from experimental measurements, see Figure 2(D). They are the integral expression of all the physicochemical phenomena leading to the formation of calcium carbonate in the process, resulting not only from the growth kinetic and its inhibition by additive, but also from other affecting phenomena. For instance: gas-liquid transfer (e.g., degassing or absorption of compounds, such as CO_2); liquid-solid reactions (e.g., dissolution or precipitation of another salt than $CaCO_3$); liquid reactions (e.g., complexation); nature of hydrodynamics (e.g., plug-flow, perfectly stirred, stagnant, presence of partial recycling); residence time distributions; turbulence intensity (affecting mass transfer); or temperature changes in the process (e.g., heating, cooling, evaporation). In the case of cooling systems, various hydrodynamic behaviors are encountered (e.g., liquid, gas-liquid, laminar, turbulent, plug-flow, nonideal) as well as gas-liquid mass transfer in cooling tower packings, with temperature changes due to heating in condenser and evaporative cooling in tower, or chemical treatments can be applied, etc.

2.4. Modeling methodology

The modeling methodology is employed here to link the local inhibition of growth kinetic of $CaCO_3$ (how much is the rate?) to the global inhibition (how much calcium deposit in the process do we avoid?); so that general knowledges obtained at phenomena scale could be used to predict various process systems.

The methodology implies to establish a local growth inhibition law from the local experimental measurements, see steps from (A) to (B) in Figure 2 and section 2.3.1. Then, the inhibition law is implemented into a process simulation software, considering all the aforementioned phenomena in addition to the sole kinetic phenomena. The results of the process simulation (step (C) in Figure 2) make it possible by comparison with the measurements also at process scale (step (D) in Figure 2 and section 2.3.2), to validate the effectiveness of the polymeric additive at the scale of the pilot plants obtained by the calcium input / output balance. Both modeling is presented below.

2.4.1. Modeling inhibition at local (kinetic) scale

As mentioned in introduction, the inhibition of growth kinetic of $CaCO_3$ is influenced by various factors, and adsorption mechanistic laws [11] allow to account for the effect of the additive concentration, the temperature, the presence of suspended solids (SS) in water, and the nature of body materials (metals and plastics in heat exchangers).

The modeling of inhibition at local (kinetic) scale therefore consists in exploiting experimental data at those scales, i.e. local rate R of formation of the $CaCO_3$ deposit and local inhibition efficiencies, to fit the parameters of the adsorption law given by equation (7), such as pre-exponential Langmuir factor (K_{ads}), adsorption energy ($\Delta E°$), and adsorption efficiency (1-b). C_{add} is the additive concentration (here HA additive).

$$\frac{R_0}{R_0 - R_{add}} = \frac{1}{1-b} + \frac{1}{(1-b)K_{ads}} \frac{1}{C_{add}} \qquad (7)$$

Based on this assumption, and on previous works performed at laboratory scale (references 7 and 11), equation (7) gives the adsorption law and the adsorption characteristics corresponding to each type of coupon having the surface previously covered by $CaCO_3$ deposit.

2.4.2. Modeling inhibition at global (process system) scale

Knowing the kinetic inhibition law, a process simulation needs to be used to predict efficiency at global (process system) scale considering other hydrodynamics, thermodynamics and chemical phenomena encountered in processes were $CaCO_3$ scaling occur. Dedicated software tools could be used depending on the application.

For industrial cooling systems studied in this work, the CooliSS (Cooling circuit Simulation Software) is used, which is a tool developed by EDF to simulate the precipitation of calcium carbonate in recirculating cooling circuit according to the design and the operating conditions of the circuit by entering some data:

- on the dimensions of the circuit: surfaces, flow rates and volumes of the various equipment;
- on the thermodynamic state of the circuit: thermal power, ambient conditions (water temperature, air temperature and humidity)
- on the quality of the river water: alkalinity, calcium hardness (THCa), conductivity, pH etc.
- on chemical treatments (acid injection in the circuit or not): location, flow rate and concentration of the injection.

From this information, the software simulates the stationary and dynamic states of the circuit, by considering the thermochemical equilibria implemented as well as the phenomena with kinetic limitation (precipitation reaction, gas-liquid transfer).

The CooliSS tool is developed under the Scilab / Xcos environment and is coupled to the PHREEQC software (DL Parkhurst and CAJAppelo, 1999) [21] for the calculation of water chemistry and to the TEFERI code (C. Bourillot, 1986) [22] for the thermal calculation in the evaporative cooling tower. Each component of the industrial cooling circuit (condenser, tanks, cooling tower, mixture) is modeled as a network of perfectly stirred reactors (CSTR, Continuous Stirred Tank Reactor). The condenser and the cooling tower are discretized in CSTR in series in order to reproduce a plug-flow behavior. The basin with the chemical additives is modeled as a single CSTR. The model uses a rate-based formulation, considering the kinetic limitation for the precipitation or dissolution of $CaCO_3$, as well as gas-liquid mass-transfer in the cooling tower for stripping as well as for the evaporation of water. More information can be found on Also-Ramos et al. [23] and Mabrouk et al. [24] for the prediction of scaling with treatments based on acid injections; and in Neveux et al. [6] for the modification of the $CaCO_3$ to account for polymeric additives.

In this work, CooliSS is used as a scale-up tool to integrate the modification of the local growth kinetic, due to the presence of polymeric additive and suspended matter, within the various conditions encountered in an industrial cooling system: hydrodynamics (nature of flows, residence time distribution), thermal conditions (temperature profiles in both the condenser and cooling tower) and materials (metals, plastics).

It is expected that implementing kinetics laws determined with local measurements within CooliSS would lead to global (system-scale) predictions of the calcium loss in compliance with experimental calcium losses measured between the make-up and the blowdown of the pilot plant, without the need to adjust phenomenological parameters (e.g., kinetic parameters) from global system information, thus validating the scale-up methodology (see Figure 2).

3. RESULTS AND DISCUSSION

3.1. Local kinetic laws (step A of Figure2)

3.1.1. $CaCO_3$ crystal growth rate on coupon surfaces during the pre-scaling phase

Table 3 gives the $CaCO_3$ growth rate on the different types of surfaces implemented in PILOT1, and PILOT 2 in the pre-scaling phase. The values are similar in both pilot plants. For stainless steel surface, the growth rates are higher, probably because of the higher condenser temperature (40°C) and the material surface specificity (stainless steel versus PVC). At reverse, the commercial PVC (CP) has very low growth rate values. This PVC has a special coating.

	$R0_{PVC\ in\ tower}$ ($mol.m^{-2}.min^{-1}$)	$R0_{CP}$ ($mol.m^{-2}.min^{-1}$)	$R0_{stainless\ steel}$ ($mol.m^{-2}.min^{-1}$)	$R0_{PVC\ in\ cold\ tank}$ ($mol.m^{-2}.min^{-1}$)
PILOT 1	$1.266\ 10^{-5}$	9.66710^{-6}	$3.987\ 10^{-5}$	$1.036\ 10^{-5}$
PILOT 2	$1.918\ 10^{-5}$	$4.971\ 10^{-6}$	$5.859\ 10^{-5}$	$1.114\ 10^{-5}$

Table 3: Local growth rates obtained by weighing the different types of coupons (equation (1)) in PILOT1 and PILOT2.

3.1.2. Effect of additive concentration on growth rate inhibition at the local scale

In a second set of experiments, a given amount of homopolymer of acrylic acid (HA) was added to the water after 9 days during which the pilots were preliminary pre-scaled. The runs were then continued during 24 days in PILOT 1 (without suspended particles) and PILOT 2 (with $100 mgL^{-1}$ of calcite particles in water). The growth rates without (R_0) and with HA addition (R_{add}) were calculated for each type of surface and the inhibition ratio η_{local} was obtained according to equation (4) at the local scale and to equation (6) at the global scale, for different HA concentrations (C_{HA}).

At the local scale, for the different types of coupons, the evolution of $1/\eta_{local}=R_0/(R_0-R_{add})$ as a function of $1/C_{HA}$, gives straight lines in the range of experimental errors (Figure 3).

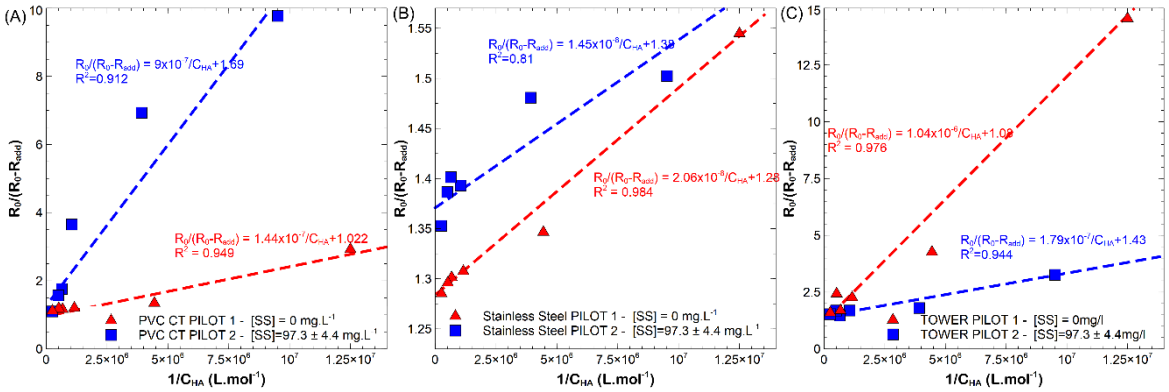

***Figure 3**: Influence of polymeric additive concentration on local crystal growth rates at the coupon scale – Adsorption of additive molecules on deposit growth sites (A) PVC coupons immersed in the cold tanks of pilots 1 and 2. (B) stainless steel coupons at the condensers outlet of pilots 1 and 2 (C) PVC coupons in the cooling tower of pilots 1 and 2.*

Regardless the nature of the coupon, the inhibition of $CaCO_3$ deposit rate at the local scale, results from the adsorption of polymeric additive molecules on the growth sites (surfaces of the coupons were already covered during the pre-scale phase of the runs). The values of the adsorption efficiency (1-b) and affinity constant K_{ads} (equation (7)) are reported in Table 4.

	Adsorption coefficients	**PVC in cold tank**	**Stainless steel**	**PVC In tower**
PILOT1	(1 – b)	0.978	0.781	0.925
	K_{ads} ($L.mol^{-1}$)	7.09 10^6 at 30°C	6.21 10^7 at 40°C	1.04 10^6 at 30°C
PILOT2	(1 – b)	0.591	0.724	0.726
	K_{ads} ($L.mol^{-1}$)	1.88 10^6 at 30°C	9.52 10^7 at 40°C	7.71 10^6 at 30°C

Table 4: Adsorption coefficients obtained with the different types of coupon materials located in PILOT1 (without suspended particles) and PILOT 2 with 100mgL^{-1} of suspended particles.

It was not possible to have a reliable measurement for commercial PVC packing (CP) because the deposit was brittle and part of the crystals were loss during weighing manipulation. Nevertheless, several observations can be made.

The comparison of stainless-steel coupons in the absence (PILOT1) and in the presence of suspended solids (PILOT2) seems to indicate that the influence of suspended solids is not significant. The efficiency factors of the polymeric additive under these conditions are of the same order of magnitude: (1 – b) = 0.781 in PILOT1 and (1 – b) = 0.724 in PILOT2.

Conversely, a strong influence of the presence of suspended solids is observed on the PVC coupon immersed in the "cold" tank of PILOT2, in which the suspended solids (SS) are brought

at a rate of 97.3 ± 4.4 mg. L^{-1}. As the contribution of SS is carried out by injection into the "cold" tank, this strong influence leads to a drastic reduction in the efficiency of the polymeric additive on the PVC coupon immersed in this "cold" tank. This low efficiency can be attributed on the one hand to the addition of SS and on the other hand to the surface condition of the coupon already covered with the deposit of $CaCO_3$ during pre-scaling phase. When no SS is added in PILOT1, the efficiency of the polymeric additive on the PVC coupon immersed in the "cold" tank is 0.978, despite the surface of the PVC coupon already covered with the $CaCO_3$ deposit.

For the PVC coupons placed in the cooling tower of each of the pilot plants, it can be seen that there is a significant difference in the efficiency of the polymer additive between the PVC coupon in PILOT2 ((1 – b) = 0.726) and that in PILOT1 ((1 – b) = 0.925). The absence of SS allowed a good efficiency of the polymeric additive.

According to the adsorption affinity constants (K_{ads}), the polymeric additive molecules seem to have a better affinity with respect to the stainless-steel coupons than for the other coupons, regardless the contribution or not of SS in pilot plants. For the PVC coupons placed in the "cold" tanks and in the atmospheric coolers of the pilot plants (towers), the affinity constants obtained are of the same order of magnitude.

The inhibition of the growth of the $CaCO_3$ deposit at the local scale of the coupons results from adsorption of the molecules of polymeric additive on the growth sites of the surface exposed to the supersaturated solution [16]. The additional presence of SS in the supersaturated solution strongly contributes to the reduction of the efficiency of the polymeric additive and therefore increases the consumption of this additive.

3.1.3 Effect of SS concentration for constant amount of HA additive at the local scale

The objective of this step is to study the influence of the SS concentration both on the calcium balances during the formation of the $CaCO_3$ deposit at the scale of the pilot plants and on the crystal growth rates at the local scale of the coupons, whose surfaces are already covered with the $CaCO_3$, at the end of step 1. The concentrations of polymeric additive HA are kept constant but different for each pilot plant: (HA) = 2 mg.L^{-1} in PILOT1and (HA) = 0.5 mg.L^{-1} in PILOT2. SS concentrations in each pilot plant vary from 20 to 300 mg.L^{-1}. During the first part of these experiments, the suspended solids used consist of 100% calcite. In the second part, the SS consists of a mass mixture of calcite (90.3%), silica (6.7%) and illite (3%).

3.1.3.1 With addition of calcite seeds

Table 5 gives the experimental values of growth rates at the local scale for the two pilot plants when only calcite seeds are added in water, for constant HA additive concentration. In this case, the two pilot plants are used to test two values of HA concentration for four different amounts of SS particles.

SS= $CaCO_3$ (100 %)					
PILOT1		**(HA) = 2.07 ± 0,10 mg.L^{-1}**			
		SS= **15.8 ± 0.4 mg.L^{-1}**	SS = **114.8 ± 5.4 mg.L^{-1}**	SS = **217.8 ± 18.7 mg.L^{-1}**	SS= **300.9 ± 16.9 mg.L^{-1}**
	R_0 initial pre-scaling (mol.m^{-2}.min^{-1})	**R_m (mol.m^{-2}.min^{-1})**	**R_m (mol.m^{-2}.min^{-1})**	**R_m (mol.m^{-2}.min^{-1})**	**R_m (mol.m^{-2}.min^{-1})**
Stainless steel	7.081 10^{-5}	5.770 10^{-5}	8.167 10^{-6}	6.791 10^{-6}	7.594 10^{-6}
PVC cold tank	1.036 10^{-5}	8.657 10^{-6}	6.580 10^{-6}	**1.548 10^{-5}**	**1.6375 10^{-5}**
PVC tower	1.049 10^{-5}	8.447 10^{-6}	5.333 10^{-6}	4.800 10^{-6}	4.630 10^{-6}
CP	7.183 10^{-6}	6.388 10^{-6}	5.638 10^{-6}	5.099 10^{-6}	4.835 10^{-6}
PILOT2		**(HA) = 0.53 ± 0.02 mg.L^{-1}**			
		SS= **18.0 ± 0.4 mg.L^{-1}**	SS = **106.5 ± 1.8 mg.L^{-1}**	SS = **203.1 ± 0.2 mg.L^{-1}**	SS = **300.2 ± 6.4 mg.L^{-1}**
	R_0 initial pre-scaling (mol.m^{-2}.min^{-1})	**R_m (mol.m^{-2}.min^{-1})**	**R_m (mol.m^{-2}.min^{-1})**	**R_m (mol.m^{-2}.min^{-1})**	**R_m (mol.m^{-2}.min^{-1})**
Stainless steel	9.090 10^{-5}	5.412 10^{-5}	1.692 10^{-5}	1.279 10^{-5}	1,358 10^{-5}
PVC cold tank	1.114 10^{-5}	1.041 10^{-5}	**1.790 10^{-5}**	**2.485 10^{-5}**	**2,564 10^{-5}**
PVC tower	1.059 10^{-5}	9.737 10^{-6}	4.688 10^{-6}	2.083 10^{-6}	1,913 10^{-6}
CP	3.324 10^{-6}	2.957 10^{-6}	2.646 10^{-6}	2.325 10^{-6}	2,121 10^{-6}

Table 5: Growth rates at the local scale on the different coupons located in different points in PILOT1 and PILOT2. SS are 100 % calcite seeds.

The results are reported in Figure 4 as well as the corresponding inhibition ratios:

• the growth rates of $CaCO_3$ on the surface of the stainless-steel coupons decrease when the SS concentration increases in the pilot plants, in the range of SS concentrations from 15 to 100 mg. L^{-1}. However, beyond SS concentration of 100 mg.L^{-1}, this influence ceases (figure 4A).

• the growth rates of $CaCO_3$ on the surface of the PVC coupons immersed in the “cold” tank are strongly influenced by the suspended solids introduced into both pilot plants. The crystal growth rates increase with increasing SS concentration. It should be remembered that the suspended solids are injected into the "cold" tanks in which these PVC coupons are immersed. This strong influence of SS leads to crystal growth rates higher than the reference rates obtained during the pre-scaling phase. Consequently, the calculation of inhibition rates is not possible for PVC coupons immersed in the "cold" tank from a certain SS concentration (figure 4B).

• for the PVC coupons placed in the air-cooling towers of the pilot plants, the crystal growth rates decrease, as for the stainless-steel coupons, when the SS concentrations increase. All the growth rates remain lower than the reference rates of PVC coupons obtained at the end of the pre-scaling stage (figure 4C).

• the growth rates of the $CaCO_3$ on the surface of commercial packing coupons (CP coupons) also decrease with increasing SS concentrations. These crystal growth rates remain lower than the reference rates obtained at the end of the pre-scaling stage (figure 4D).

The different behaviors of the coupons exposed in the cooling towers (PVC and CP), at the condenser outlet (stainless steel) and in the “cold” tanks (PVC) are attributable to the different exposure hydrodynamic regimes. In the cooling towers and the condenser outlet, the coupons are subjected to a flow regime of “plug flow” type, whereas the coupons immersed in the “cold” tanks are exposed to a perfectly stirred reactor type regime [6,7].

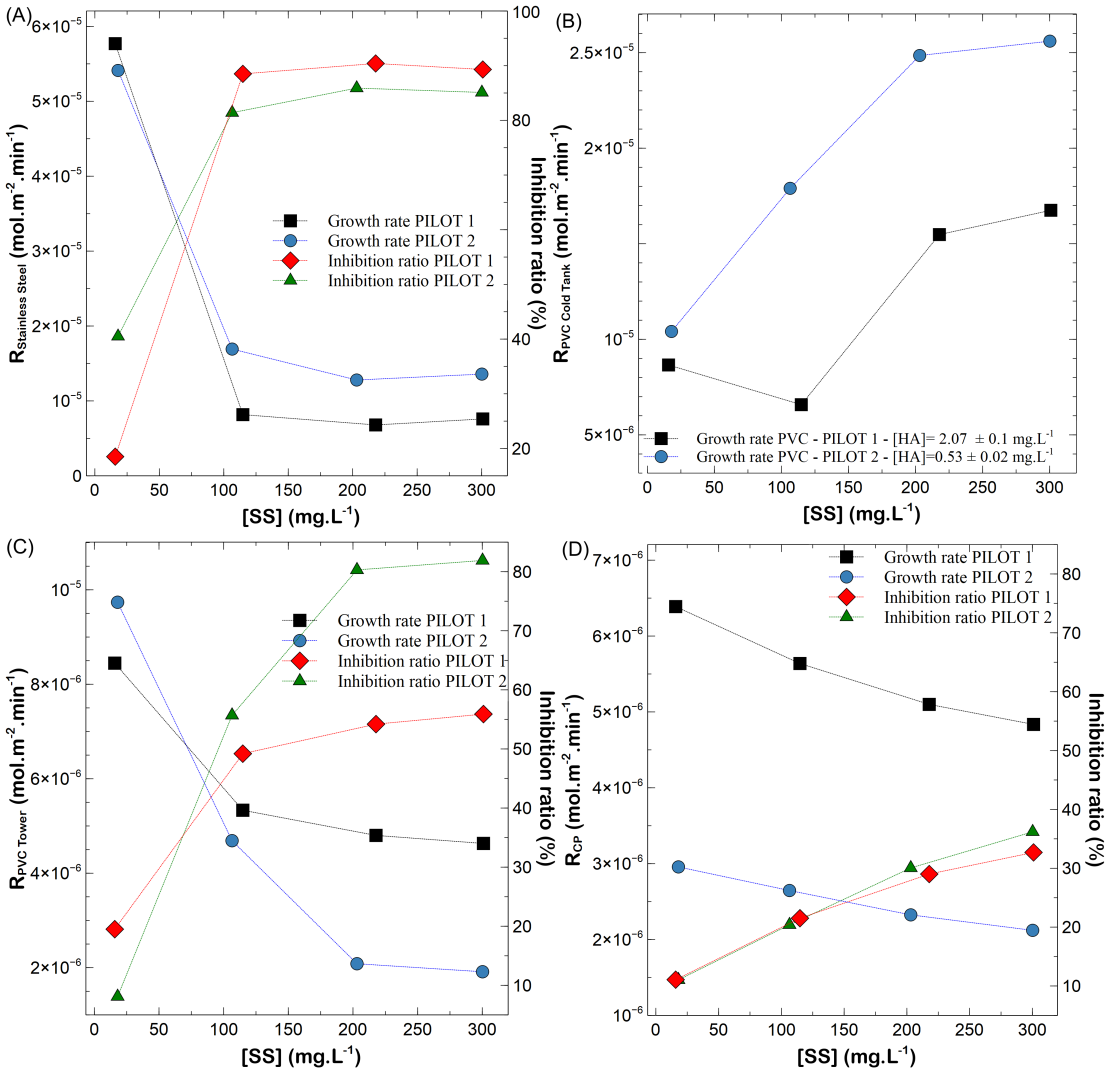

Figure 4: *$CaCO_3$ growth rates at local scale and inhibition ratios as a function of SS concentration– (A) stainless steel coupons, (B) PVC coupons in "cold" tanks, (C) PVC coupons in towers and (D) commercial packing coupons (CP)*

3.1.3.2 With addition of a mixture of calcite, silica and illite seeds

Table 6 gives the experimental values of growth rates at the local scale for the two pilot plants when a mixture of calcite, silica and illite seeds are added in water, for constant HA additive concentration. Figure 6 shows the deposit growth rates and corresponding inhibition ratios on the surface of different coupons.

SS = $CaCO_3$ (90,3 %) + SiO_2 (6,7 %) + Illite (3 %)				
PILOT1	**(HA) = 2.07 ± 0.10 mg.L^{-1}**			
	SS = 23.2 ± 5.1 mg.L^{-1}	**SS = 108.1 ± 6.3 mg.L^{-1}**	**SS = 199.6 ± 16.2 mg.L^{-1}**	**SS = 305.0 ± 13.2 mg.L^{-1}**
	R_m (mol.m^{-2}.min^{-1})	**R_m (mol.m^{-2}.min^{-1})**	**R_m (mol.m^{-2}.min^{-1})**	**R_m (mol.m^{-2}.min^{-1})**
Stainless steel	1.120 10^{-5}	7.688 10^{-6}	8.761 10^{-6}	7.027 10^{-6}
PVC cold tank	**1.452 10^{-5}**	**1.532 10^{-5}**	**1.624 10^{-5}**	**1.635 10^{-5}**
PVC tower	1.951 10^{-6}	4.762 10^{-6}	6.376 10^{-6}	7.714 10^{-6}
CP	1.467 10^{-6}	1.628 10^{-6}	1.736 10^{-6}	2.151 10^{-6}
PILOT1	**Growth inhibition ratio PILOT 1**			
Stainless steel	84.2	89.1	87.6	90.1
PVC cold tank	Growth rates higher than the reference growth rate (pre-scaling) : strong influence of SS concentration			
PVC tower	81.4	54.6	39.2	26.5
CP	79.6	77.3	75.8	70.1
PILOT2	**(HA) = 0,53 ± 0,02 mg.L^{-1}**			
	SS = 21.5 ± 0,4 mg.L^{-1}	**SS = 105.0 ± 1,8 mg.L^{-1}**	**SS = 206.9 ± 1.4 mg.L^{-1}L**	**SS = 307.1 ± 6.4 mg.L^{-1}**
	R_m (mol.m^{-2}.min^{-1})	**R_m (mol.m^{-2}.min^{-1})**	**R_m (mol.m^{-2}.min^{-1})**	**R_m (mol.m^{-2}.min^{-1})**
Stainless steel	1.281 10^{-5}	9.104 10^{-6}	4.391 10^{-6}	4.287 10^{-6}
PVC cold tank	**2.304 10^{-5}**	**2.450 10^{-5}**	**2.802 10^{-5}**	**2.864 10^{-5}**
PVC tower	2.065 10^{-6}	4.564 10^{-6}	5.747 10^{-6}	8.610 10^{-6}
CP	no weight gain	no weight gain	1.336 10^{-7}	4.302 10^{-7}
PILOT2	**Growth inhibition ratio PILOT 2**			
Stainless steel	85.9	90.0	95.2	95.3
PVC cold tank	Growth rates higher than the reference growth rate (pre-scaling) : strong influence of SS concentration			
PVC tower	80.5	56.9	45.7	18.7
CP	100	100	96.0	87.1

Table 6: Growth rates at the local scale on the different coupons located in different points in PILOT1 and PILOT2- SS are a weight mixture of $CaCO_3$ (90,3 %) + SiO_2 (6,7 %) + Illite (3 %) seeds.

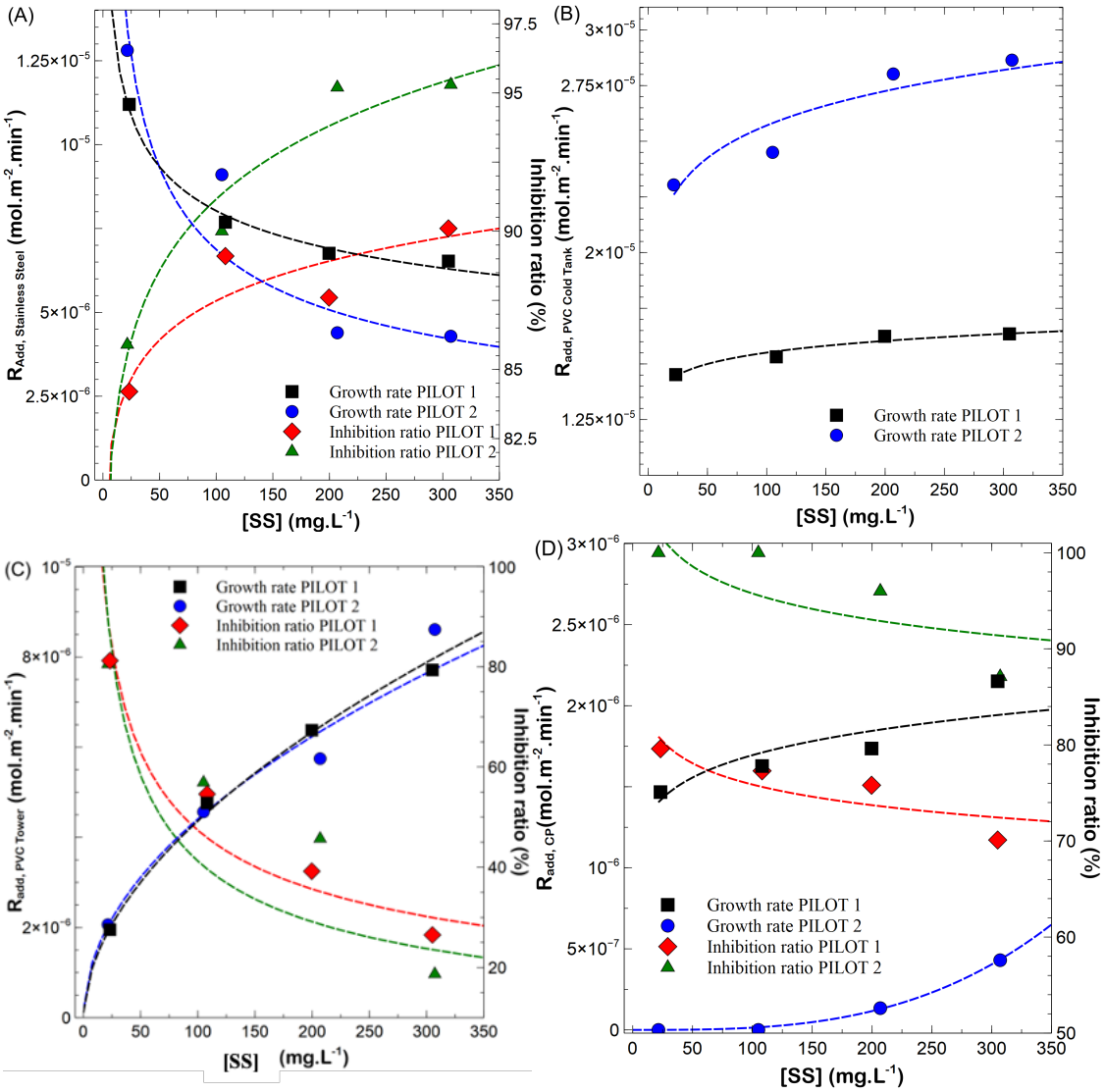

Figure 5 *- $CaCO_3$ growth rates at local scale and inhibition ratios in presence of a mixture of suspended materials – (A) stainless steel coupons, (B) PVC coupons in "cold" tanks, (C) PVC coupons in towers and (D) commercial packing coupons (CP)*

The deposit rate on the stainless-steel coupons, (as in case of 100% calcite suspended solids), does not seem to be influenced by the mixture of suspended solids brought into the pilot plants (see figure 5A). They are more sensitive to the presence of polymeric additive leading to increased inhibition ratios stabilizing around 90 to 96%.

The PVC coupons immersed in the "cold" tanks were strongly subjected to the effect of suspended solids leading to $CaCO_3$ growth rates higher than the reference rates obtained at the end of the pre-scaling phase (PILOT1: R_{0PVC} cold tank = 1.036 10^{-5} mol.m^{-2}.min^{-1}; PILOT2: $R_{0\,PVC}$ cold tank = 1.114 10^{-5} mol.m^{-2}.min^{-1}). Therefore, crystal growth inhibition ratios could not be determined for this type of coupons (Figure 5B).

For the PVC coupons located in the atmospheric cooling towers of the pilot plants, the growth rates increase with the increase of the suspended solids mixture concentration (cf. figure 5C) and the inhibition ratios (η) decrease.

For the commercial packing coupons (CP) located in the atmospheric cooling towers of the two pilot plants, the $CaCO_3$ growth rates also increase with the increase of suspended solids mixture concentration (cf. figure 5D) and the corresponding inhibition ratios decrease.

In the atmospheric coolers where the PVC coupons and the commercial packing coupons are located, we observe a different behavior compared to the tests carried out with the 100% calcite SS. Previously, the inhibition rates increase when SS concentration increases whereas in the tests carried out with the mixture of SS, the inhibition rates decrease when mixture of SS concentration increases. This difference in behavior seems to be independent of the nature of SS used during these different assays. It could be attributed to the problems of hydraulic distribution and dispersion of the solution in the atmospheric coolants. This result is also consolidated by the crystal growth inhibition ratios in the atmospheric coolant of PILOT2 which are systematically higher than those obtained in the atmospheric coolant of PILOT1, whereas the concentration of polymeric additive injected into PILOT1 (2.07 ± 0.10 mg.L^{-1}) is higher than in PILOT2 (0.53 ± 0.02 mg.L^{-1}).

The inhibition of the $CaCO_3$ deposit observed in the two pilot plants results from the adsorption of the additive molecules on the growth sites [16]. The dosage of polymeric additive in the supersaturated solution, made by spectrophotometric method (see supporting information tables S1 and S2) and in the solid deposits taken at the end of each test phase, after dissolution in acidic solution, (see supporting information tables S3 and S4) confirm that the additive molecules are adsorbed on the surface of the deposit. These results are also qualitatively consolidated by the characterization of solid deposit samples, using infrared spectroscopy in absorption mode, showing the presence of HA molecules (see Figure S1 of supporting information).

3.2 Local inhibition law

At the end of this experimental campaign carried out at a pilot scale, we have observed that the efficiency factors (1–b) obtained with the HA additive are of the same order of magnitude as those reported in the previous work of Neveux et al. [6], also obtained in a pilot plant, without SS. Moreover, at the local scale of the coupons, our results are relatively close to the values obtained with the constant composition laboratory set-up (ref 7 and 11), with calcite seeds and PVC (see Table 7).

The adsorption affinity constants (K_{ads}) depend on temperature by the relation:

$$K_{ads}(T) = K^0_{ads}(T)\,\mathrm{Exp}(-\Delta E^0/RT) \qquad (8)$$

K^0_{ads} is the pre-exponential factor of Langmuir obtained experimentally at $5.08\ 10^{-10}$ L.mol^{-1} by plotting Ln K_{ads}=f(1/RT) from the data obtained in a previous work with the device at constant composition and the adsorption device (6).

Efficiency factor **(1-b)** with HA additive				Adsorption affinity constant $\mathbf{K_{ads}}$ **(L.mol^{-1})**			Adsorption energy $\Delta\mathbf{E^0}$ (kJ.mol^{-1})	
	Laboratory Constant composition set-up (ref. 7;11)	Obtained by Coupons in Pilot plants (this work)	According to reference (6)	Laboratory Constant composition set-up (ref. 7;11)	Obtained by Coupons in Pilot plants (this work)	According to reference (6)	Laboratory Constant composition set-up (ref. 7;15)	According to reference (6)
Calcite seeds	0.980		0.970 (without SS)	3.3 10^7 to 5.1 10^7 (depending on temperature)	1.1 10^6 to 3.3 10^8 (depending on temperature)	2.6 10^7 to 8.7 10^7 (depending on temperature)	- 76.8 to - 97.8	- 91.8
Stainless steel		0.724-0.781						
PVC cold tank		0.591-(with SS) 0.978 (without SS)						
PVC tower		0.726-(with SS) 0.925 (without SS)						

Table 7: comparison of efficiency factors and affinity constants obtained in this work with previous works

Moreover, the fraction θ of growth sites on the crystals recovered by additive can be related to the affinity constant and to the additive concentration:

$$\theta = \frac{K_a C_{add}}{1 + K_a C_{add}} \qquad (9)$$

(1-b) characteristic of the efficiency of the additive lays between 0 and 1 and the growth rate in the presence of additive Ra is given by the equation:

$$R_{add} = R_0 - \theta R_0 (1 - b) \qquad (10)$$

By combining equation (9) and equation (10) an inhibition law can be obtained and directly compared to the global inhibition ratio calculated by the calcium input/output balance obtained in experiments, without (ΔCa_0) and with additive (ΔCa_{add}). This law was then implemented in CooliSS Software for calculation of input-output calcium content in the pilot plants.

$$\eta_{local}(T) = \frac{R_0 - R_{add}}{R_0} = (1 - b)\frac{K^0_{ads} e^{(-\Delta E^0/RT)} C_{add}}{1 + K^0_{ads} e^{(-\Delta E^0/RT)} C_{add}} \qquad (11)$$

3.3 Global calcium balance at the pilot scale (step D of figure 2)

Together with the local measurements of kinetic inhibition on coupons during the experimental campaign, water flow rate and calcium contents were measured at the water input (feeding the cooling circuit) and output (blowdown of the circuit), in order to calculate the global calcium balance according to equation (5) and associated global inhibition efficiency according to equation (6).

Experimental results are reported in Table 8 for the various experimental conditions depending on the nature and concentration of suspended solids, as well as additive concentration. Temperature evolution along the circuit was kept identical (from 30 to 40°C) during all the assays.

First campaign: effect of additive (HA) concentration at constant SS (calcite) concentration						
Nature of SS	SS : (calcite)	HA (mg/L)	**Calcium balance PILOT 1 (mol.L^{-1})**	SS : (calcite)	HA (mg/L)	**Calcium balance PILOT 2 (mol.L^{-1})**
	0	0	$2.17\ 10^{-3} \pm 3.71\ 10^{-4}$	0	0	$2.14\ 10^{-3} \pm 3.69\ 10^{-4}$
SS : calcite	0	0.16 ± 0.02	$1.98\ 10^{-3} \pm 1.29\ 10^{-4}$	97.31 ± 4.37	0.21 ± 0.01	$1.93\ 10^{-3} \pm 0.24\ 10^{-4}$
		0.45 ± 0.03	$8.51\ 10^{-4} \pm 0.85\ 10^{-4}$		0.51 ± 0.00	$9.66\ 10^{-4} \pm 1.06\ 10^{-4}$
		1.73 ± 0.29	$1.15\ 10^{-3} \pm 1.19\ 10^{-4}$		1.91 ± 0.12	$1.33\ 10^{-3} \pm 2.04\ 10^{-4}$
		2.97 ± 0.13	$1.31\ 10^{-3} \pm 1.22\ 10^{-4}$		3.10 ± 0.49	$1.43\ 10^{-3} \pm 1.55\ 10^{-4}$
		3.88 ± 0.03	$1.23\ 10^{-3} \pm 1.00\ 10^{-4}$		4.03 ± 0.05	$1.53\ 10^{-3} \pm 1.77\ 10^{-4}$
		7.85 ± 0.25	$1.04\ 10^{-3} \pm 1.43\ 10^{-4}$		7.99 ± 0.19	$1.49\ 10^{-3} \pm 0.79\ 10^{-4}$
Second campaign: effect of SS (calcite and mixture) concentration at constant additive (HA) concentration						
Nature of SS	SS (mg/L)	HA (mg/L)	**Calcium balance PILOT 1 (mol.L^{-1})**	SS (mg/L)	HA (mg/L)	**Calcium balance PILOT 2 (mol.L^{-1})**
	0	0	$1.86\ 10^{-3} \pm 2.62\ 10^{-4}$	0	0	$1.81\ 10^{-3} \pm 3.85\ 10^{-4}$
SS : calcite	15.8 ± 0.8	2.08 ± 0.10	$1.10\ 10^{-3} \pm 0.00$	18.0 ± 0.4	0.53 ± 0.03	$1.22\ 10^{-3} \pm 2.21\ 10^{-4}$
	114.8 ± 5.4		$1.23\ 10^{-3} \pm 1.97\ 10^{-4}$	106.5 ± 1.8		$1.52\ 10^{-3} \pm 2.53\ 10^{-4}$
	217.8 ± 18.7		$1.13\ 10^{-3} \pm 1.25\ 10^{-4}$	203.1 ± 0.2		$1.59\ 10^{-3} \pm 0.04\ 10^{-4}$
	300.9 ± 16.9		$1.10\ 10^{-3} \pm 0.00$	300.2 ± 6.4		$1.68\ 10^{-3} \pm 0.90\ 10^{-4}$
SS : 90.3 % calcite + 6.7 % silica + 3.0 % Illite	23.2 ± 5.1		$1.15\ 10^{-3} \pm 0.14\ 10^{-4}$	21.5 ± 0.4		$1.28\ 10^{-3} \pm 0.25\ 10^{-4}$
	108.1 ± 6.3		$1.12\ 10^{-3} \pm 0.64\ 10^{-4}$	105.0 ± 1.8		$1.30\ 10^{-3} \pm 0.58\ 10^{-4}$
	199.6 ± 16.2		$1.01\ 10^{-3} \pm 0.91\ 10^{-4}$	206.9 ± 1.4		$1.20\ 10^{-3} \pm 1.42\ 10^{-4}$
	305.0 ± 13.2		$1.07\ 10^{-3} \pm 0.85\ 10^{-4}$	307.1 ± 6.4		$1.37\ 10^{-3} \pm 0.59\ 10^{-4}$

Table 8: Calcium balances measured in PILOT1 and PILOT2 with various additive concentrations (HA), nature and concentration of suspended solids (SS), for a temperature range along cooling circuit between 30°C (cold sections) and 40°C (hot sections).

First, it can be observed that both pilots show similar calcium balance over two time periods; for example, for baseline conditions without additive and suspended solids (between 1.81 10^{-3} mol.L^{-1} and 2.17 10^{-3} mol.L^{-1}); and for conditions with about 2 mg/L additive and 100 mg/L calcite (around 1.30 10^{-3} mol.L^{-1}). Considering the experimental uncertainties (concentration

measurements and fluctuations during the time period), results can be considered as repeatable over time and reproductible between the two pilots.

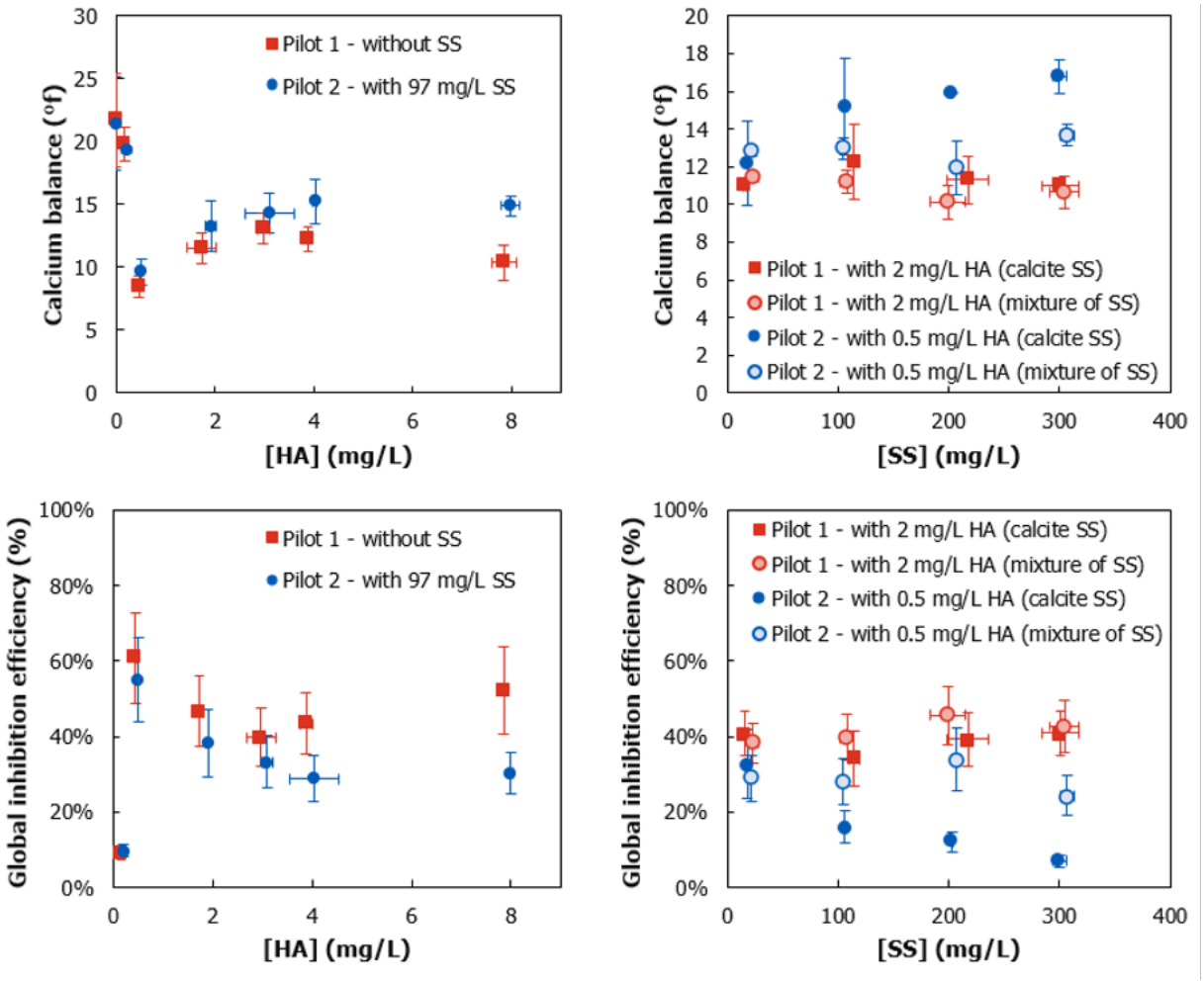

Figure 6 *–Calcium balances at global scale (top) and global inhibition efficiency (bottom). Left: first experimental campaign exhibiting the effect of homopolymer of acrylic acid (HA) in two pilots without and with suspended solids (SS) respectively. Right: second experimental campaign exhibiting the effect of the concentration of suspended solids (SS).*

The individual effects are displayed on Figure 6 (with data from Table 8), showing the influence of additive and suspended solids concentration on both the calcium balance and the global inhibition efficiency. As explained in the methodology section, global inhibition results not only from the local inhibition of crystal-growth, but also from other rate-controlled and thermodynamic phenomena (hydrodynamics, mass-transfer, multiphase equilibria, temperature changes, etc). Tendencies can then be less distinct as they could be at local scale. Results are nevertheless in compliance with tendencies observed in previous works on pilot plants [6, 24] and local results of this work. They can be summarized as follows:

Effect of HA. While increasing the additive concentration, a sharp decrease of calcium balance (i.e. increase of inhibition efficiency) is observed, followed by a stabilization (see Figure 6,

left). This is consistent with local measurements (see Figure 3) and is a consequence of the adsorption mechanism behind inhibition of crystal-growth. It means that a small quantity of additive will rapidly result in a decrease of the calcium deposit, but that the efficiency cannot be improved even with large quantities of additives. Depending on the water hardness and process operating conditions, the use of HA may therefore be sufficient to totally avoid scaling (e.g., soft water, low F_{VC}, low temperature), but a complementary treatment such as acid injection may be required for harder conditions (e.g., hard water, high F_{VC}, high temperature).

Effect of SS (concentration and nature). The presence of SS in water decreases the global inhibition, as observed locally. Locally, coupons on PVC cold tank show inhibitions reduced by around 40% due to the presence of 100 mg/L of calcite SS (1-b factor from 0.978 to 0.591); but the decrease is far less stiff at global scale (Figure 6, left, see the differences between pilots). The effect of SS concentration is also less visible in the presence of both calcite SS and HA at 2 $mg.L^{-1}$ (Figure 6, right, see data of pilot 1 and filled points of pilot 2). A clear tendency is however obtained if little HA is used (0.5 $mg.L^{-1}$) and mixture of SS other than calcite (Figure 6, right, pilot 2). In this case, one assumption could be that HA preferably adsorbs on other solids than calcite (illite, SiO_2) leading to the consumption of a small quantity of HA not available for adsorption on calcite, hence a decrease in efficiency.

Effect of flows. For both effects, differences between local and global efficiencies are systematically observed. For example, for about 4 $mg.L^{-1}$ of HA and without suspended solids, a global inhibition efficiency around 40% is obtained (see Figure 6), whereas the local efficiency in similar conditions is around 80%. This is interpreted as an effect of the nature of flows in the cooling circuit, as highlighted before [6]. The presence of HA and/or SS in water affects the crystal-growth kinetic, which needs to be integrated along the water flows in order to retrieve the evolution of concentration at various locations in the process. Flows being mostly of plug-flow type in heat-exchangers (condenser, cooling tower), the concentration follows a logarithmic evolution. Hence, we have a nonlinear dependency between local (kinetic) inhibition and global (concentration balance) inhibition.

Overall, these experimental results at global scale exhibit the measurable consequence of using HA to reduce $CaCO_3$ scaling in representative process conditions, which is affected obviously by the inhibition of growth kinetic but also by other phenomena: a 70% local inhibition obtained at lab-scale will not lead to a global 70% inhibition at global scale (rather around 25% in the case of cooling circuits). It means that local phenomenological information such as kinetic data, measured at lab-scale or with coupons, needs to be considered together with other phenomena occurring in the process, for instance using a process simulation model. This is the object of the last section.

3.4 From local to global scale: comparison between experimental and simulated inhibition efficiencies (step C)

In this final step, the aim is to scale-up results obtained at local scale to predict global (process system scale) inhibition efficiency using a process phenomenological model, in order to use generic knowledge independent of process system to any process with calcium carbonate deposition issues, as long as operating parameters (concentrations, temperature) are in similar ranges. The process model helps to consider all parameters influencing the $CaCO_3$ growth and

its inhibition, such as temperature (heating and cooling); materials (heat exchangers, gas-liquid contactors, pipes, basins); and concentrations of calcium, carbonates, additive and suspended solids (depending on the chemistry in the upstream flows, multiphase transfer, mixing and recycling). Therefore, the local inhibition efficiency largely fluctuates depending on the location in the cooling circuit (for instance, see Figure 7), in addition to fluctuating to exogen parameters (raw water, meteorology) and applied chemical treatments. The procedure is explained for cooling circuits but should be applicable for other industrial systems with similar conditions.

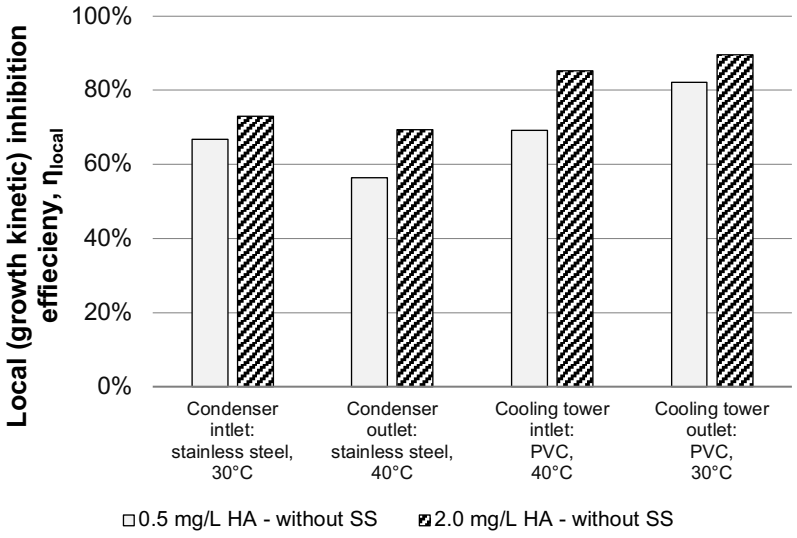

***Figure 7** – Example of local inhibition efficiency calculated with equation (11) for several locations in the cooling circuit, various materials and temperature*

Knowing the local kinetics, the CooliSS model is used to integrate all rate-controlled phenomena (heat transfer, water evaporation, residence time distributions etc.) to calculate the evolution of concentrations within the pilot plant. The input parameters are the one from the local inhibition law, i.e. the Langmuir's pre-exponential factor ($K°_{ads}$) 5.08 10^{-10} $L.mol^{-1}$, obtained by laboratory constant composition set-up; the experimental efficiency factor (1 – b), which depends on the material (location within the cooling circuit) and the presence/absence of suspended solids (SS), with values for condenser stainless steel from 0.724 to 0.781 obtained by stainless steel coupons weighing, and for cooling tower PVC from 0.591 in the presence SS to 0.978 in the absence of SS obtained by PVC coupons weighing; and the adsorption energy (ΔE^0) from -97.8 to -76.8 $kJ.mol^{-1}$, obtained by laboratory constant composition set-up. One parametrized, the model can be used to simulate all concentrations, and consequently the calcium "loss" by mass balance, using the process operating conditions: make-up, blowdown and evaporation flow rates; temperatures of the solution at the condenser outlet and in the atmospheric cooler; and physico-chemical properties of the water (total alkalimetric degree, calcium hydrotimetric degree, conductivity, pH, Cl^- concentration, dissolved oxygen concentration, polymeric additive and SS concentrations).

Figure 8 shows an example of comparison between the water calcium balance obtained on pilot plant 1 and pilot plant 2 and the corresponding simulations with CooliSS software, in which equation (11) was implemented.

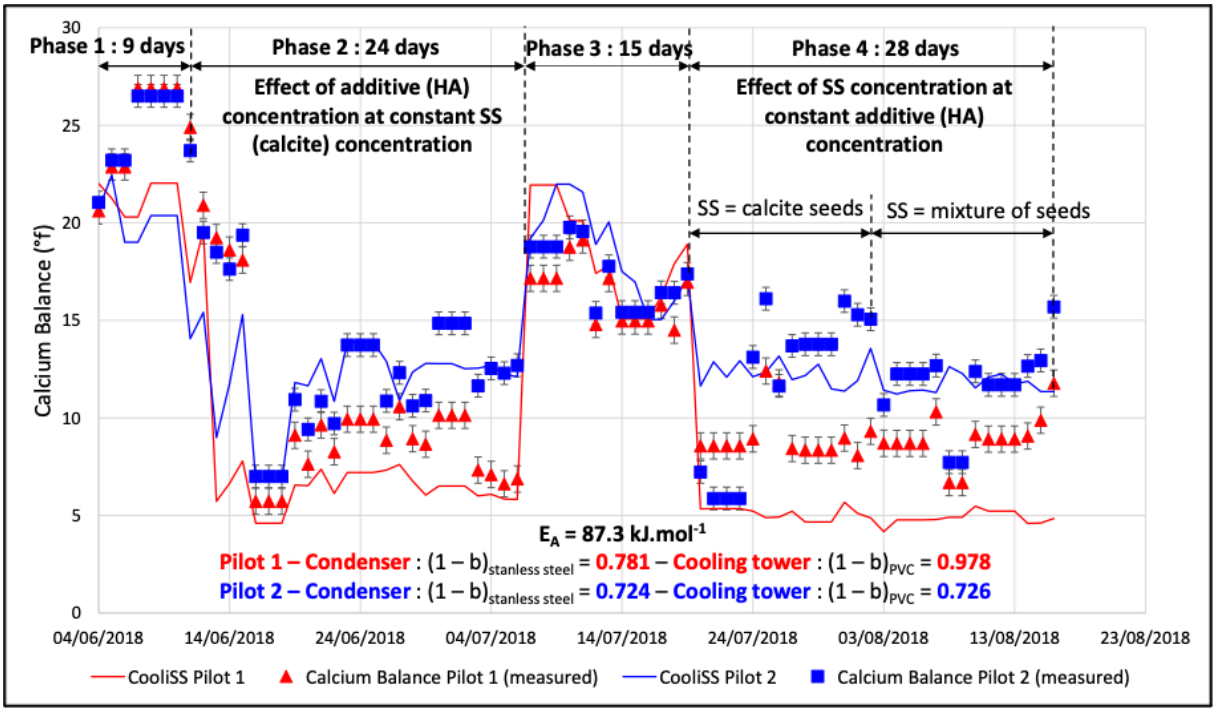

***Figure 8**: Comparison of calcium loss in water measured in the pilots and simulated with CooliSS software – Phase 1 and phase 3 correspond to the cycles of pre-scaling of pilots and coupons.*

It can be observed from figure 8, that the model fits very well the calcium balance evolution in the absence of SS. The presence of SS decreases the efficiency. It is worth re-mentioning that no fitting parameters is used here. The scale-up methodology is validated, as only information at local (phenomenological) scale are used and able to predict global (process system) scale performances. Meaning that all phenomena concomitant to the kinetic ones seem to be proper modeled, as seen before [6].

4. CONCLUSION

In this work, scaling experiments were carried out in semi-industrial pilot plants, feeding them with a solution of controlled composition at a supersaturation ratio of 7.6. The tests were organized with two factors of interest: concentration of polymeric additive and concentration and nature of suspended particles. Between each variable studied, the pilot installations were pre-scaled intentionally, in order to reduce the duration of the tests.

From the $CaCO_3$ growth kinetic data obtained in the constant composition device and from the immersed coupons in the pilot plants, a local inhibition law of the growth of $CaCO_3$ deposit was proposed. This local law contains three main components: the experimental efficiency factor (1 – b) specific to the material constituting the exchange body (stainless steel for the condenser tubes and PVC for the packing in the cooler), the adsorption affinity constant K^0_{ads} dependent on temperature and on adsorption energy ΔE^0 and the concentration of polymeric additive C_{add}.

This law was implemented in the CooliSS software, simulating the calcium balances in the pilot plants. We have been able to highlight the sensitivity of the CooliSS software to the efficiency factors of the materials. Improving the sensitivity of the inhibition model including the variation of SS concentration and nature, we have demonstrated the main variables influencing the use of this model to explore other operational conditions of industrial cooling circuits.

We found that the model succeeds in reproducing the variations in calcium balance resulting from the addition of polymeric additives in the pilot plants. However, compared to experimental data we have observed a lack of sensitivity of the model regarding the variation of SS concentration. It could be attributed to the absence of an additional corrective term in the local law used. Thus, the next step will be an improvement on this model in order to identify another additional corrective factor linking the efficiency factors of these materials to the SS concentration as well as to the nature of these SS.

Supporting information. spectrophotometric dosage of polymeric additive in liquid and solid phases and infrared spectroscopy on solid deposit.

This information is available free of charge via the Internet at http://pubs.acs.org/.

References

(1) Ramírez-García P., Duran-Olivencia M.A., Kellermeier M.,Van Driessche A.E.S.. Determining the operational window of green antiscalants: A case study for calcium sulfate. Desalination, 2022, vol.544, 116128.

(2) Cruz C., Cisternas L.A., Kraslawski A., Scaling problems and control technologies in industrial operations:Technology assessment. Separation and Purification Technology, 2018,vol.207, 20–27.

(3) Singh Y. B., Ng K.C., Elucidation of dual-mode inhibition mechanism of a typical polymer-based antiscalant on Red seawater for thermal desalination at higher temperatures and higher concentration factors. Journal of Petroleum Science and Engineering, 2019, vol.183, 106380.

(4) Mohammadi Z., Rahsepar M. The use of green Bistorta Officinalis extract for effective inhibition of corrosion and scale formation problems in cooling water system. Journal of Alloys and Compounds, 2019, vol.770, 669-678.

(5) Ahmadi S., Khormali A., Fridel Meerovich Khoutoriansky. Optimization of the demulsification of water-in-heavy crude oil emulsions using response surface methodology. Fuel, 2022, vol.323, 12427.

(6) Neveux T., Bretaud M., Chhim N., Shakourzadeh K., Rapenne S., “Pilot plant experiments and modeling of $CaCO_3$ growth inhibition by the use of antiscalant polymers in recirculating cooling circuits” Desalination, 2016, vol.397, 43-52.

(7) Chhim N., Haddad E., Neveux T., Bouteleux C., Teychené S., Biscans B. “Performance of green antiscalants and their mixtures in controlled calcium carbonate precipitation conditions reproducing industrial cooling circuits”. Water Research, November 2020, vol.186, 116334.

(8) Chaussemier, M.; Pourmohtasham, E.; Gelus, D.; Pécoul, N.; Perrot, H.; Lédion, J.; Cheap-Charpentier, H.; Horner, O.; “State of Art of Natural Inhibitors of Calcium Carbonate Scaling. A Review Article”. Desalination 2015, vol.356, 47−55.

(9) Hasson, D.; Shemer, H.; Sher, A. State of the Art of Friendly “Green” Scale Control Inhibitors: A Review Article. Ind. Eng. Chem. Res. 2011, vol.50 (12), 7601−7607.

(10) Lisitsin D., Hasson D., Semiat R., Modeling the effect of anti-scalant on $CaCO_3$ precipitation in continuous flow, Desalin. Water Treat., 2009, vol. 1, 17–24.

(11) Chhim N., Kharbachi C., Neveux T., Bouteleux C., Teychene S., Biscans B.; « Inhibition of calcium carbonate crystal growth by organic additives using the constant composition method”. Journal of Crystal Growth, 2017, vol. 472, 35-45.

(12) Liu D., «Research on performance evaluation and anti-scaling mechanism of green scale inhibitors by static and dynamic methods,» PhD manuscript, HAL Id: pastel-00637079, Ecole Nationale Supérieure d'Arts et Métiers, 2011.

(13) Li H., «Mineral precipitation and deposition in cooling systems using impaired waters : mechanisms, kinetics, and inhibition,» Ph.D. thesis, University of Pittsburgh, Pittsburgh, 2010.

(14) Cavano R.R., «Inhibitor choice & dosage (for scale control in cooling towers),» Paper presented at the Corrosion conference Houston Texas (paper no. 05063), 2005.

(15) He S., Kan A.T., Tomson M.B., «Inhibition of calcium carbonate precipitation in NaCl brines from 25 to 90°C» Applied Geochemistry,1999, vol. 14, 17-25.

(16) He S., Kan A.T., Tomson M.B., «Inhibition of mineral scale precipitation by polymers,» in Water Soluble polymers. Solutions Properties and Applications, Z. Amjad, Ed., 1998,163-171.

(17) Fergusson R.J., Fergusson B.R., Stancavage R.F., «Modeling scale formation and optimizing scale inhibitor dosages in Membrane Systems» paper presented at the AWWA Membrane Technology Conference, 2011.

(18) Vanderpool D., «Calculating minimum threshold inhibitor dosage,» The Analyst, the voice of the water treatment industry, vol. XII (3), 2006.

(19) Jafa Mazumder M.A.“A review of green scale inhibitors: process, types, mechanism and properties”. Coatings 2020, vol.10, 928-956.

(20) Liu D., Dong W., Li F., Hui F ;, Ledion J. « Comparative performance of polyepoxysuccinoc acid and polyaspartic acid on scaling inhibition by static and rapide controlled precipitation methods” Desalination 2012, vol.304, 1-10.

(21) Parkhurst D.L. and Appelo C.A.J., «User’s guide to PHREEQC (version 2)-a computer program for speciation, batch reaction, one-dimensional transport and inverse geochemical calculations,» 1999.

(22) Bourillot C., «TEFERI, Modèle numérique pour le calcul des performances d'un réfrigérant atmosphérique humide,» Internal report EDF - H-T30-1977-00965-FR, 1977).

(23) Alos-Ramos O., Shakourzadeh K.,Thomas C., Lacombe J.M., Vermeeren D., Soreau S., CooliSS (Cooling circuit Simulation Software): a computer program to simulate the water chemistry in recirculating cooling water circuits, Conference at the Nuclear Plant Chemistry (NPC) Conference, Berlin, Germany, 2008.

(24) Mabrouk A., Neveux T., Rapenne S., Alos-Ramos O., Shakourzadeh K., Modelling scale formation in wet cooling system and validation with pilot plant data, Conference at the 10th European Congress of Chemical Engineering, Nice, France, 2015. http://dx.doi.org/10.13140/RG.2.1.2374.3602.

TABLE OF CONTENTS (TOC)